AMERICAN ACADEMY OF OPHTHALMOLOGY®

Genotype- and Phenotype-Based Subgroups in Geographic Atrophy Secondary to Age-Related Macular Degeneration

The EYE-RISK Consortium

Marc Biarnés, MPH, PhD,[1,2] Johanna M. Colijn, MD, MSc,[3,4] Jose Sousa, PhD,[5] Lucia L. Ferraro, MD,[1,2] Míriam Garcia, OD, MSc,[1,2] Timo Verzijden, MSc,[3,4] Magda A. Meester-Smoor, PhD,[3,4] Cécile Delcourt, PhD,[6] Caroline C.W. Klaver, MD, PhD,[3,4,7,8] Anneke I. den Hollander, PhD,[9,10] Imre Lengyel, PhD,[5] Tunde Peto, MD, PhD,[11] Jordi Monés, MD, PhD,[1,2] on behalf of the EYE-RISK Consortium

Purpose: Geographic atrophy (GA) secondary to age-related macular degeneration is considered a single entity. This study aimed to determine whether GA subgroups exist that can be defined by their genotype and phenotype.

Design: Retrospective analysis of cross-sectional data.

Participants: Individuals (196 eyes of 196 patients) 50 years of age or older with GA from the EYE-RISK database.

Methods: Participants were graded for the presence of each of the following fundus features on color fundus photography: large soft drusen, reticular pseudodrusen (RPD), refractile drusen, hyperpigmentation, location of atrophy (foveal vs. extrafoveal), and multifocal lesions. Genotypes of 33 single nucleotide polymorphisms previously assigned to the complement, lipid metabolism, or extracellular matrix (ECM) pathways and *ARMS2* also were included, and genetic risk scores (GRSs) for each of those 3 pathways were calculated. Hierarchical cluster analysis was used to determine subgroups of participants defined by these features. The discriminative ability of genotype, phenotype, or both for each subgroup was determined with 10-fold cross-validated areas under the receiver operating characteristic curve (cvAUCs), and the agreement between predicted and actual subgroup membership was assessed with calibration plots.

Main Outcome Measures: Identification and characterization of GA subgroups based on their phenotype and genotype.

Results: Cluster analyses identified 3 subgroups of GA. Subgroup 1 was characterized by high complement GRS, frequently associated with large soft drusen and foveal atrophy; subgroup 2 generally showed low GRS, foveal atrophy, and few drusen (any type); and subgroup 3 showed a high *ARMS2* and ECM GRS, RPD, and extrafoveal atrophy. A high discriminative ability existed between subgroups for the genotype (cvAUC, $\geq$0.94), and a modest discriminative ability existed for the phenotype (cvAUC, $<$0.65), with good calibration.

Conclusions: We identified 3 GA subgroups that differed mostly by their genotype. Atrophy location and drusen type were the most relevant phenotypic features. *Ophthalmology Retina 2020;4:1129-1137 © 2020 by the American Academy of Ophthalmology. This is an open access article under the CC BY-NC-ND license (http://creativecommons.org/licenses/by-nc-nd/4.0/).*

Supplemental material available at www.ophthalmologyretina.org.

See Editorial on page 1125.

Geographic atrophy (GA) is the advanced form of dry age-related macular degeneration (AMD) and affects approximately 5 million people worldwide.[1] It is characterized by progressive loss of retinal pigment epithelium (RPE), adjacent photoreceptors, and choriocapillaris.[2] Areas affected by GA correlate with deep scotomas: when the fovea is involved, a marked loss in visual acuity ensues, but vision is severely affected even without foveal involvement because of the presence of perifoveal scotomas that affect the ability to read, drive, or recognize faces.[3]

Currently, no treatment exists for GA, and recent clinical trials have shown disappointing results.[4–6] Potential reasons for these unsuccessful attempts include inappropriate therapeutic targets, dosages, timing of intervention, or even inadequate trial populations.[7] Thus, a better understanding of GA is needed to develop rational therapies.

https://doi.org/10.1016/j.oret.2020.04.014
ISSN 2468-6530/20

It is conceivable that different mechanisms lead to a similar phenotype, namely, RPE atrophy and photoreceptor loss in patients 50 years of age or older who already have deposits (drusen) on the posterior pole. However, if the molecular mechanism by which disease develops is different among subgroups of GA patients, a "one-size-fits-all" therapeutic approach is unlikely to be successful, and switching to development of targeted therapies would be required.[8] Specific combinations of genetic variants may lead to GA by affecting different molecular pathways, which, in turn, may induce a set of characteristic fundus features. This combination of features would identify disease subgroups, whereas genotype–phenotype correlations would provide insights into disease mechanisms that eventually lead to targeted therapies. These subgroups also may have prognostic (natural course of the disease) and predictive (response to treatment) value. Therefore, evaluating the potential existence of disease subgroups clearly is relevant.

Several methods exist to identify subgroups within a population. One of them is cluster analysis, in which subgroups (clusters) are created so that the observations in a given cluster are more similar to each other than to those in other clusters.[9] One appeal of this method is that it is data driven and therefore, less prone to bias. The purpose of this study was to determine whether subgroups of participants with GA exist based on fundus features and genotype. Then, genotype–phenotype correlations within each subgroup were evaluated.

Methods

Design

This was a retrospective analysis of the EYE-RISK database version 6.0, which collected and harmonized information from European studies with epidemiologic data on common eye diseases, including AMD (ALIENOR; Coimbra Eye Study; CORRBI; Crescendo-3C; Creteil Study; EPIC; EUGENDA; EUREYE; GAIN; HAPIEE; MARS; Montrachet; PAMDI; POLA; Rotterdam Studies 1, 2 and 3; Thessaloniki Eye Study; and Tromsø Eye Study). Most of them were population-based epidemiologic studies, and details have been published previously.[10] The EYE-RISK database was developed to create a single reference that included all other studies. This facilitated the required structure to allow data science to explore it through correlation, which is one of the approaches to understand the data and relies heavily on integration and dimensionality. All studies followed the tenets of the Declaration of Helsinki and were approved by the local ethics committees (GAIN: Hospital Quirón Teknon Ethics Committee; Rotterdam Studies: the Medical Ethics Committee of the Erasmus Medical Center and the review board of The Netherlands Ministry of Health, Welfare and Sports; ALIENOR: Comité de Protection des Personnes Sud-Ouest et Outre-Mer III), and all participants provided informed consent.

Eligibility Criteria

Geographic atrophy was defined on color fundus photography (CFP) as well-defined areas of 175 μm or more in diameter of RPE loss through which choroidal vessels were visible. Participants of either gender who were 50 years of age or older with GA in either eye documented at least 1 visit in the EYE-RISK database and with graded CFP images for the features of interest were eligible. Eyes with prior or concomitant neovascular AMD, scarring, other causes of RPE atrophy (high myopia, inherited retinal degenerations, etc.), other concomitant retinal disorders, or poor CFP image quality were excluded. In bilateral cases, the study eye was chosen randomly.

Study Procedures

The input for the cluster analyses were selected fundus features to represent the phenotype and pathway-based genetic risk scores (GRSs) to represent the genotype. Pathway-based GRSs were used as proxies for the possible underlying disease mechanisms. Fundus features were graded per eye by experienced graders or clinicians in their corresponding studies in accordance with international classifications.[11] These features, defined by the presence of these characteristics on CFP within the Early Treatment Diabetic Retinopathy Study grid, were selected for their potential relevance and adequate grading on CFP: (1) large soft drusen (≥125 μm), presence of at least 1 soft druse with a smallest diameter at least as large as the diameter of a retinal vein in the disk margin[12]; (2) reticular pseudodrusen (RPD), yellowish subretinal lesions arranged in a network (i.e., reticular) pattern 125 to 250 μm in width[13]; (3) refractile (calcified, crystalline) drusen, 1 or more drusen with deposition of yellowish-white glistening material beneath the retina[14]; (4) hyperpigmentation, the presence of multiple small brown hyperpigmented lesions; (5) foveal atrophy, the absence of RPE in the geometric center of the foveal avascular zone; and (6) multifocal lesions, more than 1 area of well-circumscribed RPE loss.

Refractile drusen and multifocal lesions were graded in all included participants at the Institut de la Màcula, Barcelona, Spain. In those participants for whom spectral-domain (SD) OCT, fundus autofluorescence, or near-infrared images were available (21 participants in the Rotterdam studies, 23 in ALIENOR, and 21 in GAIN), these also were used to determine the phenotype. In these cases, RPD were defined on SD OCT as granular hyperreflective deposits located between the RPE and the ellipsoid zone; on fundus autofluorescence as numerous spots of reduced autofluorescence with brighter lines in between; and on near-infrared images as hyporeflective lesions on a hyperreflective background in regular patterns.[13] Graders were masked to the GRS.

Genotyping

The genotyping of AMD-associated genetic variants in the Rotterdam Studies was carried using the Illumina 550K, 550k due/610K Illumina arrays (Illumina, Inc., San Diego, CA). Sequencing was performed at an average depth of ×54 using the Nimblegen SeqCap EZ V2 capture kit (Roche, Basel, Switzerland) on an Illumina Hiseq2000 sequencer using the TrueSeq version 3 protocol. The sequence reads were aligned to human genome build 19 using the Burrows-Wheeler Aligner. Afterward, the aligned reads were processed further using Picard's MarkDuplicates, SAMtools, and the Indel Realignment and Base Quality Score Recalibration tools from the Genome Analysis Toolkit (Broad Institute, Cambridge, MA). Genetic variants were called using the HaplotypeCaller from the same platform. Samples with low concordance with genotyping array (<95%) or differing 4 standard deviations or more from the mean on the number of detected variants per sample, transition to transversion ratio of high heterozygote to homozygote ratio, and low call rate (<90%) were discarded. Single nucleotide variants with a low call rate (<90%) and out of Hardy-Weinberg equilibrium ($P < 10^{-8}$) also were removed.[15] In ALIENOR, genotype was imputed using the 1000 Genomes Project (March 2012) and the Haplotype Reference

Consortium reference panel (release 1.1). Genotyping of the GAIN cohort was performed by using single-molecule molecular inversion probes and next-generation sequencing. SAMtools was used for genotyping calling. Variants with a coverage of less than ×40, deviation from Hardy-Weinberg equilibrium, and a low genotyping concordance with previously performed genotyping were filtered out. Further details of this genotyping platform are described elsewhere (de Breuk et al, unpublished data, 2020).

Genetic risk scores were calculated only for participants with available information on 5 major risk alleles: rs570618 and rs10922109 (*CFH*), rs3750846 (*ARMS2*), rs429608 (*CFB/C2*), and rs2230199 (*C3*). If this information was available for a given individual, then GRSs were calculated for 3 different pathways previously associated with AMD: the complement pathway, lipid metabolism, and extracellular matrix (ECM) remodeling.[16] The genes included in each GRS were taken from Fritsche et al[16] and are shown in Table 1, and the corresponding rs numbers of the single nucleotide polymorphisms (SNPs) are provided in Table S1 (available at www.ophthalmologyretina.org). Genetic allele dosages were annotated as 0 for noncarriers, 1 for heterozygotes, and 2 for homozygotes and were imputed when missing (see "Statistical Analysis"). If direct genotyping was unavailable, we used the exact dosage (continuous value from 0–2) from imputations instead. If no imputation data were available, we checked the availability of genotyping data for a proxy SNP (one in high linkage disequilibrium with that particular SNP).[16] If no direct genotyping or imputation data were available for a proxy SNP (or a proxy SNP could not be found at all), the genotype was set to missing.

Each GRS was calculated for each participant as the sum of the product of each genetic allele dosage for each SNP by its β coefficient (as reported by Fritsche et al[16]) in the log-odds scale and resulted in the generation of 1 GRS for the complement pathway, 1 for the lipids, and 1 for the ECM, besides the *ARMS2* SNP for each participant.[16]

Statistical Analysis

For descriptive purposes, univariate analyses used the mean (standard deviation) or median (interquartile range [IQR]) as appropriate for quantitative variables and number (percentage) for categorical variables. An agglomerative hierarchical cluster analyses with Euclidean distance and average linkage was used to determine the groupings between the different variables. The agglomerative method begins with all observations as their own cluster and forms progressively larger groups by adding nonclustered observations to a group. The Euclidean distance measures the shortest distance between 2 points in space (i.e., a straight line), and the average linkage uses the mean distance of observations between subgroups as the proximity measure between them.[9] All quantitative variables were standardized (converted to variables with means of 0 and standard deviations of 1) to minimize scaling issues. The Calinski-Harabasz method was used to determine the optimal number of groups. The features were compared between clusters using the Kruskal-Wallis test for quantitative variables and the Fisher exact test for categorical variables. The characteristic features of each group were determined by inspection of their main attributes. These analyses also were replicated in participants from the Rotterdam Study, who made the largest contribution to sample size.

To test the robustness of the results, a different cluster method was used: *k* means. *k* (the number of subgroups) was determined from the results of the hierarchical method. The percent of patients classified in the same subgroups by the 2 approaches was determined, and the features of subgroups in concordant cases were compared.

The discriminating ability of the main features (genotype, phenotype, or both) for classification of individual eyes into each GA subgroup was assessed using cross-validated areas under the receiver operating characteristic curve (cvAUCs) and their corresponding receiver operating characteristic (ROC) curves based on 10-fold cross-validated logistic regression models, adjusted for age and gender. Ten-fold cross-validation is a statistical resampling method to correct for overfitting (optimistic estimates of performance)[17]: the sample is divided randomly in 10 groups, the model is fit on 9 of them, and predictions are made in the left-out subsample; this process is repeated 10 times, each time using a different subsample for prediction, and the final cvAUC is the mean of the 10 calculated areas under the ROC curves. Model calibration (the agreement between the predicted and the actual classification into a specific GA subgroup) was assessed graphically with calibration plots.

Statistical analyses were conducted using Stata IC software version 15.1 (StataCorp, College Station, TX) and R software version 3.6.1 (R Foundation for Statistical Computing, Vienna,

Table 1. Genes Included for Derivation of Each Genetic Risk Score

Assumed Pathway	Genes Used to Calculate the Genetic Risk Score
Complement	*C3*, *C9*, *CFH*, *CFB/C2*, *CFI*, *TMEM97/VTN*
Lipids	*ABCA1*, *APOE*, *CETP*, *LIPC*
Extracellular matrix	*ADAMTS9*, *COL4A3*, *COL8A1*, *SYN3/TIMP3*, *VEGF-A*
ARMS2	*ARMS2*

Table 2. Baseline Characteristics of Patients.

Features	Values
Demographic	
Age (yrs)	
Mean (SD)	82.4 (7.2)
Range	56.9–97
Female gender, no. (%)	121 (61.7)
Right eye, no. (%)	99 (50.5)
Phenotypic, no. (%)	
Large soft drusen (≥125 μm)	90 (45.9)
Reticular pseudodrusen	66 (33.7)
Refractile drusen	48 (24.5)
Hyperpigmentation	136 (69.4)
Foveal atrophy	98 (50.0)
Multifocal lesions	120 (61.2)
Genetic risk scores	
Complement	
Mean (SD)	0.67 (1.03)
Range	−3.15 to 2.85
Lipids	
Mean (SD)	−0.03 (0.23)
Range	−0.79 to 0.49
Extracellular matrix	
Mean (SD)	−0.04 (0.20)
Range	−0.56 to 0.61
ARMS2	
Mean (SD)	0.81 (0.73)
Range	0–2.15

SD = standard deviation.
The values for the genetic variables represent the genetic risk score.

Table 3. Subgroups within Geographic Atrophy as Determined from Cluster Analysis for the Overall Sample and for the Sample from the Rotterdam Study

	Overall (n = 188)				Rotterdam Study (n = 126)			
	Subgroup 1 (n = 115 [61.2%])	*Subgroup 2 (n = 21 [11.2%])*	*Subgroup 3 (n = 52 [27.7%])*	P *Value*	*Subgroup 1 (n = 40 [31.8%])*	*Subgroup 2 (n = 56 [44.4%])*	*Subgroup 3 (n = 30 [23.8%])*	P *Value*
Soft drusen ≥125 µm	58 (50.4)	7 (33.3)	20 (38.5)	0.18	28 (70.0)*	32 (57.1)†	7 (23.3)‡	**<0.001**
RPD	32 (27.8)†	3 (14.3)‡	28 (53.9)*	**0.001**	5 (12.5)†	5 (8.9)‡	10 (33.3)*	**0.02**
Refractile drusen	35 (30.4)	6 (28.6)	7 (13.5)	0.06	11 (27.5)	18 (32.1)	5 (16.7)	0.31
Hyperpigmentation	75 (65.2)	17 (81.0)	39 (75.0)	0.26	28 (70.0)	37 (66.1)	24 (80.0)	0.44
Foveal atrophy	60 (52.2)†	16 (76.2)*	20 (38.5)‡	**0.013**	27 (67.5)*	32 (57.1)†	10 (33.3)‡	**0.02**
Multifocal lesions	72 (62.6)	11 (52.4)	34 (65.4)	0.60	22 (55.0)	36 (64.3)	18 (60.0)	0.65
GRS								
Complement	1.16 (1.07)*	0.30 (1.08)†	0.14 (1.71)‡	**0.0001**	1.57 (1.03)*	1.05 (0.99)†	0.03 (1.41)‡	**0.0001**
Lipids	0.05 (0.20)*	−0.46 (0.16)‡	−0.07 (0.25)†	**0.0001**	−0.14 (0.34)†	0.14 (0.19)*	−0.21 (0.29)‡	**0.0001**
ECM	−0.10 (0.23)‡	−0.08 (0.10)†	0.13 (0.22)*	**0.0001**	−0.08 (0.22)†	−0.14 (0.24)‡	0.13 (0.27)*	**0.0001**
ARMS2	1.08 (1.08)*	0 (1.08)‡	1.08 (1.08)*	**0.0001**	0.0 (1.08)‡	1.08 (0.0)*	1.08 (1.08)*	**0.0001**

ECM = extracellular matrix; GRS = genetic risk score; RPD = reticular pseudodrusen.
Values represent median (interquartile range) for quantitative variables and number (%) for categorical variables. Values for GRS are shown in the original scale (unstandardized) to ease interpretation. Boldface values represent statistically significant results. Percentages may not add up to 100% because of rounding.
*Highest value for each statistically significant feature.
†Middle value for each statistically significant feature.
‡Lowest value for each statistically significant feature.

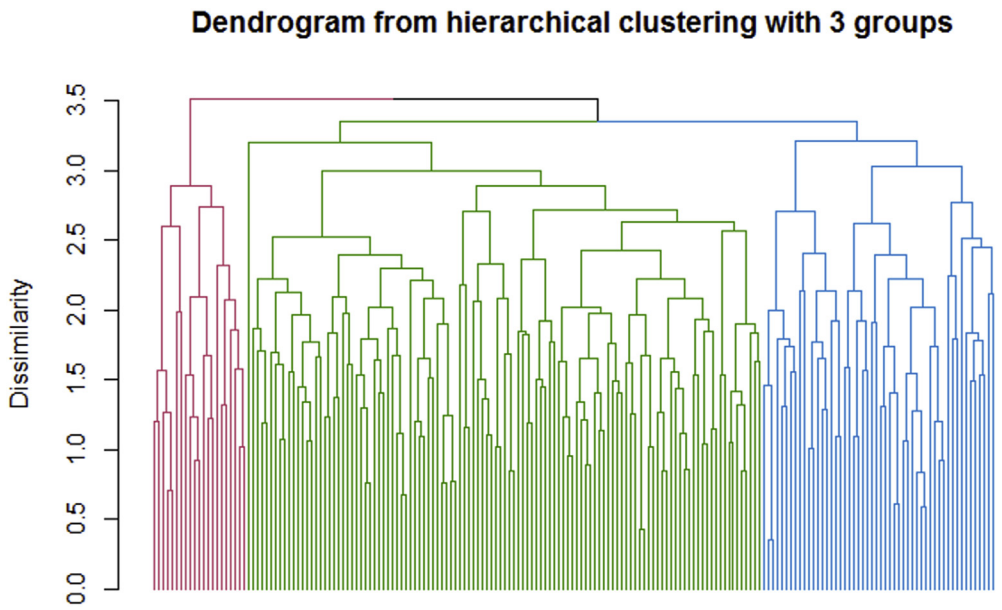

Figure 1. Dendrogram showing hierarchical cluster analysis. The vertical axis represents a measure of dissimilarity. In the horizontal axis, each eye is represented by a vertical line starting at the bottom of the figure, and they progressively form clusters with other similar eyes (based on genotype and fundus features), represented by short horizontal lines. Subgroup 1 is green, subgroup 2 is red, and subgroup 3 is blue.

Austria). A 2-tailed *P* value of 0.05 or less was considered statistically significant.

Results

We identified 196 participants (196 eyes) meeting eligibility criteria: 132 participants from the Rotterdam Study 1, 2, and 3; 43 from ALIENOR; and 21 from GAIN (Tables S2 and S3, available at www.ophthalmologyretina.org). The descriptive features of all participants are shown in Table 2.

Eight participants consistently formed their own small clusters and were excluded. The analysis was performed on the remaining 188 eyes. The subgroups identified by hierarchical cluster analyses are shown in Table 3, and the corresponding dendrogram in Figure 1. The optimal number of clusters was 3, with a similar median age in each subgroup (83.3 years [IQR, 8.4 years], 83.3 years [IQR, 9.0 years], and 82.0 years [IQR, 9.6 years] in clusters 1, 2 and 3, respectively; $P = 0.58$). The values for the GRS were back-transformed to its original scale to ease interpretation (i.e., unstandardized). The cluster with the highest value for the complement and lipid-based GRS was subgroup 1, that for the ECM-based GRS was subgroup 3, and those for *ARMS2* were subgroups 1 and 3. Similar results were obtained using *k* means as the clustering method (see Table S4, available at www.ophthalmologyretina.org), with the same category assigned to each participant by both methods in 87.2% of cases (Table S5, available at www.ophthalmologyretina.org). When the comparisons between subgroups were restricted to these cases,

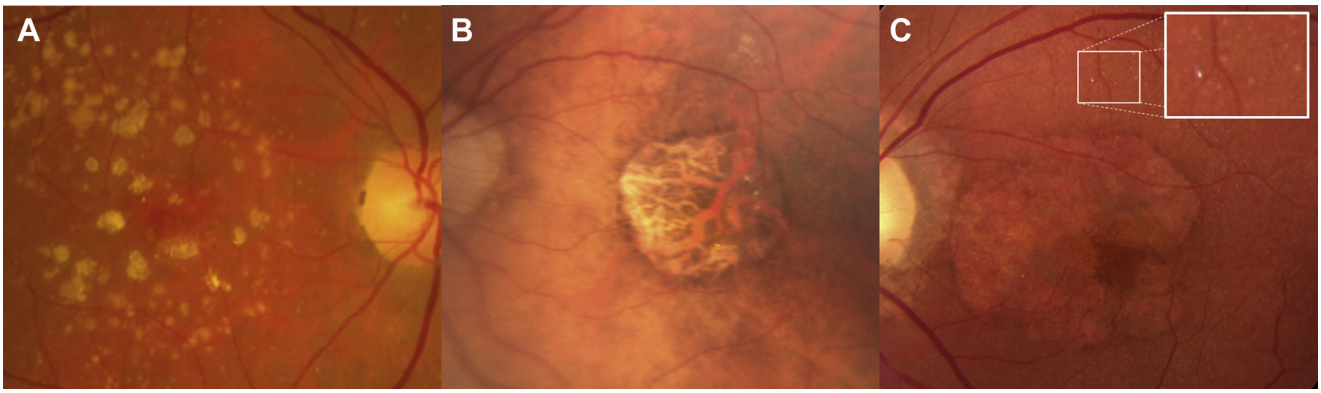

Figure 2. Fundus photographs showing each phenotype derived from hierarchical cluster analysis. **A**, Subgroup 1, with foveal atrophy and large soft and refractile drusen, had the highest complement genetic risk score (GRS). **B**, Subgroup 2, with foveal atrophy and few drusen of any type, generally had a low GRS. **C**, Subgroup 3, with extrafoveal areas of atrophy and reticular pseudodrusen (insert), had the highest median value for the extracellular matrix-based GRS and *ARMS2*.

Table 4. Discriminating Ability between Each Subgroup versus All Others of All Fundus Features Combined (Phenotype), all Genetic Risk Scores and the *ARMS2* Variant (Genotype), and Both (Phenotype plus Genotype)

Subgroup	Variables	Cross-Validated Area under the Receiver Operating Characteristic (95% Confidence Interval)	*P* Value
1	Phenotype	0.55 (0.51–0.59)	<0.0001
	Genotype	0.96 (0.93–0.98)	
	Both	0.95 (0.91–0.98)	
2	Phenotype	0.64 (0.54–0.73)	<0.0001
	Genotype	0.95 (0.92–0.99)	
	Both	0.96 (0.94–0.99)	
3	Phenotype	0.63 (0.53–0.72)	<0.0001
	Genotype	0.94 (0.92–0.98)	
	Both	0.96 (0.92–0.98)	

All models were adjusted for age and gender.

the results were similar (Table S6, available at www.ophthalmologyretina.org). When the analysis was conducted in patients from the Rotterdam Study (the largest contributor to the study sample), the distribution of cases in each category and the features in subgroup 2 differed, whereas those in subgroups 1 and 3 were similar to other analyses (Table 3). Representative CFP images of each subgroup are shown in Figure 2.

The ability of the genotype, phenotype, or both to discriminate among GA subgroups is shown in Table 4, and the corresponding ROC curves are shown in Figure 3A. The genotype cvAUC was excellent for each subgroup (cvAUC, 0.94–0.96), whereas the phenotype showed a modest discriminating ability (cvAUC, 0.55–0.64). These results suggest that subgroups were genotype driven.

Given the combined information (genotype plus phenotype), the calibration plots (Fig 3B) show the agreement between the predicted (x-axis) and observed (y-axis) frequencies of belonging to each subgroup. These plots show prespecified deciles of propensity of being classified into subgroup X (hollow circles) for subgroup 1, with the largest sample, and tertiles for subgroups 2 and 3, with smaller sample sizes. The locally weighted scatterplot smoothing line (in blue) for these circles should be as close as possible to the diagonal line, which indicates perfect agreement between predicted and observed classification into a given subgroup. The results showed good agreement, but the sample size was small to derive consistent conclusions for subgroups 2 and 3.

Discussion

Using a combination of phenotype and genotype, 3 GA subgroups were observed. Subgroup 1 was characterized by a high median GRS for the complement; a high median GRS for the lipids, foveal atrophy, or large soft drusen also were found frequently in most analyses. Subgroup 2 was less consistent, with generally low to moderate values for all GRSs, foveal atrophy, and few drusen (any type). Subgroup 3 showed the highest GRS for the ECM and *ARMS2*, high RPD load, and extrafoveal lesions. These patterns generally

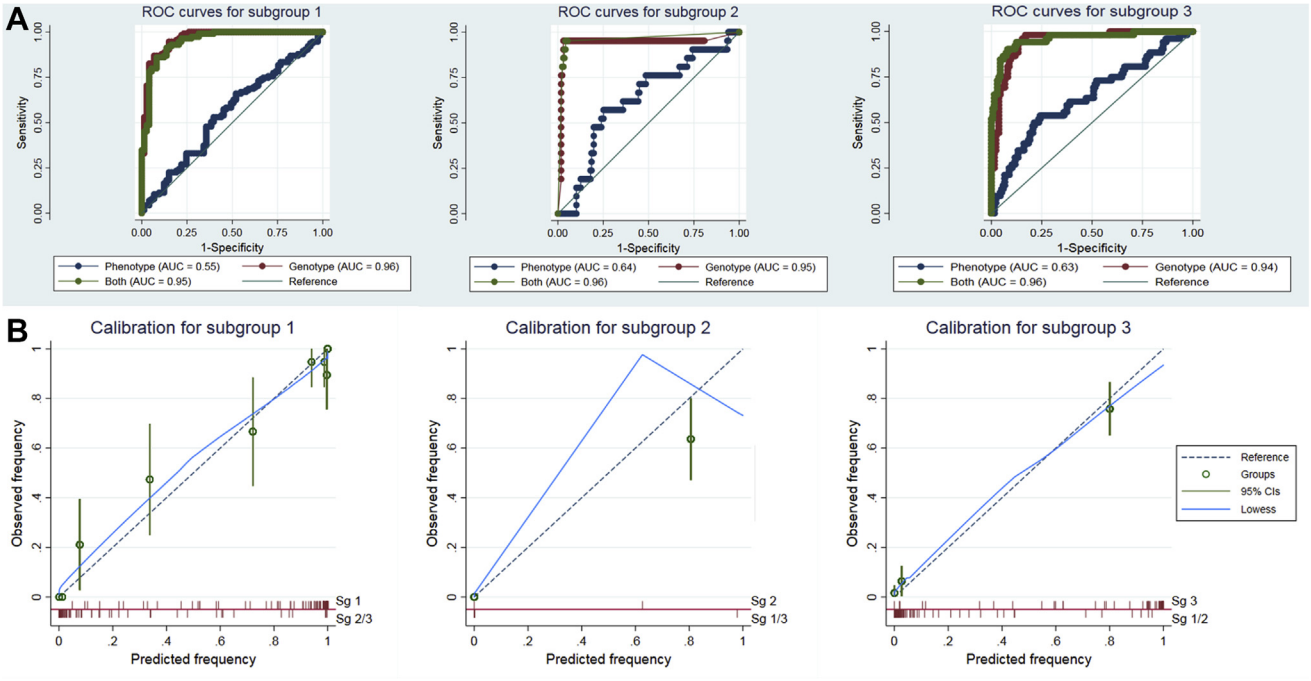

Figure 3. Receiver operating characteristic (ROC) curves and calibration plots. **A**, Receiver operating characteristic curves for the genotype, phenotype, and both for subgroup 1 (left), subgroup 2 (center), and subgroup 3 (right) showing very high ROC curves for the genotype and the combined (genotype plus phenotype) features. **B**, Calibration plots for subgroup 1 (left), subgroup 2 (center), and subgroup 3 (right). Predictions are close to observed membership. AUC = area under the receiver operating characteristic curve; CI = confidence interval; Sg = subgroup.

were robust to the clustering method and the subpopulation evaluated.

Subgroups were driven largely by the GRS, as shown by their higher discriminative ability as compared with the phenotypic features (cvAUC, $P < 0.0001$; Table 4; Fig 3A). Therefore, the phenotype guided subgroup membership only modestly. Calibration plots Fig 3B) showed good results (particularly for subgroup 1, with the largest size), suggesting that belonging to a determined subgroup can be predicted fairly well as soon as genotype and phenotype are known. These results were obtained through 10-fold cross-validation, thus providing a likely estimate of performance on new samples.

It is also interesting to evaluate potential genotype–phenotype correlations within subgroups. In subgroup 1, with a high complement GRS, most cluster analyses also showed that a high proportion of patients demonstrated large soft drusen (≥125 μm) and foveal atrophy. Other features were distributed similarly between subgroups. Another study based only on patients in the GAIN cohort (ClinicalTrials.gov identifier, NCT01694095) used multimodal imaging (including fundus autofluorescence and SD OCT) but no genetic data to identify GA endophenotypes. Three subgroups that differed in terms of drusen type and atrophy location were found.[18] Kersten et al[19] found that AMD carriers of rare *CFH* variants showed a fundus characterized by larger drusen area, drusen with crystalline appearance (refractile drusen), and drusen nasal to the disc. Thus, the known relationship between soft drusen load and complement activation in AMD[19–21] also may occur in GA.

Subgroup 2 demonstrated the most variable results. In the entire sample and with both clustering methods, it was characterized by low GRS, few drusen, and foveal atrophy. It has been reported that approximately 5% of cases of dry AMD actually harbor a mutation associated with a known inherited retinal degeneration.[22] This raises the possibility that some eyes in this subgroup do not actually have GA. This is a source of concern in GA trials, too. These results were not found in the Rotterdam sample (Table 3), as discussed below.

For subgroup 3, a high GRS for the ECM and *ARMS2* was related to RPD and extrafoveal atrophy. Reticular pseudodrusen usually present an extrafoveal topographic distribution,[23] and GA tends to grow in areas of RPD,[24] explaining the relationship between these fundus features. The relationship between RPD and genetic variants has been evaluated in different studies. A recent meta-analysis found that the *ARMS2* SNP conferred an increased risk of AMD with RPD as compared with AMD without RPD.[25] The *AREDS2* reported a higher GRS and prevalence of *ARMS2* risk alleles in RPD as compared with non-RPD cases, with borderline statistically significant differences for the *C3* and *CFH* risk alleles.[26] However, none of these studies analyzed the genetic differences between patients with prevalent GA by RPD status. This study confirmed the relationship between RPD and *ARMS2*. Reticular pseudodrusen have been associated with changes in the choroid, Bruch's membrane, and RPE, but a direct link between these lesions and specific SNP in the ECM pathway has not been reported previously and must be confirmed. Of note, Pool et al[27] recently reported just 2 clusters underlying AMD molecular pathologic features using a systems biology approach: parainflammation (with complement genes) and ECM homeostasis (with *ARMS2*), similar to findings in subgroups 1 and 3, respectively.

The patterns observed for subgroups 1 and 3 emerged across clustering methods and samples and were the most consistent results of this study. Hierarchical and *k* means analyses were very similar, with nearly 90% of cases classified in the same categories by both methods. As previously mentioned, the analysis in the sample from the Rotterdam Study revealed differences with the overall sample regarding the percent of cases in each subgroup and in the characteristics of subgroup 2, with a high GRS for the lipids and *ARMS2*. They may be the result of chance or may reflect true differences across samples, grading methods, or both. Cases in subgroup 2 may be more heterogeneous or may have mixed characteristics between those in subgroups 1 and 3, and thus may be more difficult to differentiate with this approach. Some features showed inconsistent findings across analyses (i.e., the lipids GRS), suggesting that they do not characterize any subgroup and that they may represent nonspecific disease mechanisms.

Refined phenotyping will require improvements in grading protocols to avoid random measurement error in risk factors. These can attenuate relationships with the outcome (regression dilution bias).[28] Replacing binary or categorical classifications with actual quantification of lesions is desired, and it is now possible with soft drusen using SD OCT. Machine learning-based algorithms are being developed for automatic RPD detection and quantification using multimodal imaging.[29] Inclusion of microvascular data from OCT angiography and fluorescence lifetime imaging ophthalmoscopy of specific features and peripheral lesions identified on ultra-widefield imaging are promising new tools for improving patient stratification.

An important limitation of the study is that different study sites used different graders and instrumentation to capture and classify phenotypic features, resulting in potential inconsistencies in classification. In addition, fundus features were defined solely on CFP; a multimodal approach would allow classification of additional relevant features. A different selection of features (functional tests, omics data, etc.) may lead to different clusters. Also, many of these fundus features are dynamic (RPD may disappear, multifocal lesions may become unifocal and vice versa, etc.), which underscores the complexities in identification of consistent and relevant subgroups. Cluster analysis can classify different stages of the disease as subgroups; we believe this is unlikely to be the case here because median age was similar across groups and certain features are irreversible (i.e., foveal atrophy cannot become extrafoveal). Working with a larger sample of incident GA patients followed up prospectively would minimize this problem, but the study would need to be enormous to identify new cases of the disease. Finally, the results need to be validated in other populations and by other researchers. Until then, these results must be regarded as exploratory.

In summary, based on a combination of fundus features and GRS, we identified 3 subgroups of patients with GA, 2

of them with consistent features. These subgroups may provide new insights into GA pathogenesis and could contribute to developing research strategies for therapies targeting specific disease pathways for different subgroups.

References

1. Wong WL, Su X, Li X, et al. Global prevalence of age-related macular degeneration and disease burden projection for 2020 and 2040: a systematic review and meta-analysis. *Lancet Glob Health*. 2014;2:e106–e116.
2. Bhutto I, Lutty G. Understanding age-related macular degeneration (AMD): relationships between the photoreceptor/retinal pigment epithelium/Bruch's membrane/choriocapillaris complex. *Mol Aspects Med*. 2012;33:295–317.
3. Sunness JS, Rubin GS, Applegate CA, et al. Visual function abnormalities and prognosis in eyes with age-related geographic atrophy of the macula and good visual acuity. *Ophthalmology*. 1997;104:1677–1691.
4. Holz FG, Sadda SR, Busbee B, et al. Efficacy and safety of lampalizumab for geographic atrophy due to age-related macular degeneration. *JAMA Ophthalmol*. 2018;136:666–677.
5. Jaffe GJ, Schmitz-Valckenberg S, Boyer D, et al. Randomized trial to evaluate tandospirone in geographic atrophy secondary to age-related macular degeneration: the GATE Study. *Am J Ophthalmol*. 2015;160:1226–1234.
6. Yehoshua Z, de Amorim Garcia Filho CA, Nunes RP, et al. Systemic complement inhibition with eculizumab for geographic atrophy in age-related macular degeneration: the COMPLETE Study. *Ophthalmology*. 2014;121:693–701.
7. Guymer RH. Geographic atrophy trials: turning the ship around may not be that easy. *Ophthalmol Retina*. 2018;2:515–517.
8. Trusheim MR, Berndt ER, Douglas FL. Stratified medicine: strategic and economic implications of combining drugs and clinical biomarkers. *Nat Rev Drug Discov*. 2007;6:287–293.
9. Everitt B, Landau S, Leese M, Stahl D. *Cluster Analysis*. 5 ed. Wiley; 2011.
10. Colijn JM, Buitendijk GHS, Prokofyeva E, et al. Prevalence of age-related macular degeneration in Europe. *Ophthalmology*. 2017;124:1753–1763.
11. Klaver CC, Assink JJ, van Leeuwen R, et al. Incidence and progression rates of age-related maculopathy: the Rotterdam Study. *Invest Ophthalmol Vis Sci*. 2001;42:2237–2241.
12. Ferris FL, Wilkinson CP, Bird A, et al. Clinical classification of age-related macular degeneration. *Ophthalmology*. 2013;120:844–851.
13. Buitendijk GHS, Hooghart AJ, Brussee C, et al. Epidemiology of reticular pseudodrusen in age-related macular degeneration: The Rotterdam Study. *Invest Opthalmol Vis Sci*. 2016;57:5593–5601.
14. Oishi A, Thiele S, Nadal J, et al. Prevalence, natural course, and prognostic role of refractile drusen in age-related macular degeneration. *Invest Opthalmol Vis Sci*. 2017;58:2198–2206.
15. Amin N, Jovanova O, Adams HH, et al. Exome-sequencing in a large population-based study reveals a rare Asn396Ser variant in the LIPG gene associated with depressive symptoms. *Mol Psychiatry*. 2017;22:537–543.
16. Fritsche LG, Igl W, Bailey JNC, et al. A large genome-wide association study of age-related macular degeneration highlights contributions of rare and common variants. *Nat Genet*. 2016;48:134–143.
17. James G, Witten D, Hastie T, Tibshirani R. *An Introduction to Statistical Learning: with Applications in R*. New York: Springer; 2017.
18. Monés J, Biarnés M. Geographic atrophy phenotype identification by cluster analysis. *Br J Ophthalmol*. 2018;102:388–392.
19. Kersten E, Geerlings MJ, den Hollander AI, et al. Phenotype characteristics of patients with age-related macular degeneration carrying a rare variant in the complement factor H gene. *JAMA Ophthalmol*. 2017;135:1037–1044.
20. Landowski M, Kelly U, Klingeborn M, et al. Human complement factor H Y402H polymorphism causes an age-related macular degeneration phenotype and lipoprotein dysregulation in mice. *Proc Natl Acad Sci*. 2019;116:3703–3711.
21. Seddon JM, Reynolds R, Rosner B. Peripheral retinal drusen and reticular pigment: association with CFHY402H and CFHrs1410996 genotypes in family and twin studies. *Invest Ophthalmol Vis Sci*. 2009;50:586–591.
22. Kersten E, Geerlings MJ, Pauper M, et al. Genetic screening for macular dystrophies in patients clinically diagnosed with dry age-related macular degeneration. *Clin Genet*. 2018;94:569–574.
23. Steinberg JS, Fleckenstein M, Holz FG, Schmitz-Valckenberg S. Foveal sparing of reticular drusen in eyes with early and intermediate age-related macular degeneration. *Invest Opthalmol Vis Sci*. 2015;56:4267–4274.
24. Marsiglia M, Boddu S, Bearelly S, et al. Association between geographic atrophy progression and reticular pseudodrusen in eyes with dry age-related macular degeneration. *Invest Ophthalmol Vis Sci*. 2013;54:7362–7369.
25. Jabbarpoor Bonyadi MH, Yaseri M, Nikkhah H, et al. Association of risk genotypes of ARMS2/LOC387715 A69S and CFH Y402H with age-related macular degeneration with and without reticular pseudodrusen: a meta-analysis. *Acta Ophthalmol*. 2018;96:e105–e110.
26. Domalpally A, Agrón E, Pak JW, et al. Prevalence, risk, and genetic association of reticular pseudodrusen in age-related macular degeneration: Age-Related Eye Disease Study 2 report 21. *Ophthalmology*. 2019;126:1659–1666.
27. Pool FM, Kiel C, Serrano L, Luthert PJ. Repository of proposed pathways and protein-protein interaction networks in age-related macular degeneration. *NPJ Aging Mech Dis*. 2020;6, 2:1–11.
28. Hutcheon JA, Chiolero A, Hanley JA. Random measurement error and regression dilution bias. *BMJ*. 2010;340.c2289–c2289.
29. van Grinsven MJ, Buitendijk GHS, Brussee C, et al. Automatic identification of reticular pseudodrusen using multimodal retinal image analysis. *Invest Ophthalmol Vis Sci*. 2015;56:633–639.

Footnotes and Financial Disclosures

Originally received: December 9, 2019.
Final revision: March 29, 2020.
Accepted: April 14, 2020.
Available online: May 1, 2020. Manuscript no. ORET-2019-324.

[1] Barcelona Macula Foundation, Barcelona, Spain.

[2] Institut de la Màcula, Hospital Quirón Teknon, Barcelona, Spain.

[3] Department of Ophthalmology, Erasmus Medical Center, Rotterdam, The Netherlands.

[4] Department of Epidemiology, Erasmus Medical Center, Rotterdam, The Netherlands.

[5] The Wellcome-Wolfson Institute for Experimental Medicine, Queens University Belfast, Belfast, United Kingdom.

[6] Inserm, Bordeaux Population Health Research Center, Université de Bordeaux, Bordeaux, France.

[7] Department of Ophthalmology, Radboud University Medical Center, Nijmegen, The Netherlands.

[8] Institute of Molecular and Clinical Ophthalmology, Basel, Switzerland.

[9] Department of Ophthalmology, Donders Institute for Brain, Cognition and Behaviour, Radboud University Medical Center, Nijmegen, The Netherlands.

[10] Department of Human Genetics, Donders Institute for Brain, Cognition and Behaviour, Radboud University Medical Center, Nijmegen, The Netherlands.

[11] Centre for Public Health, Queen's University Belfast, Belfast, United Kingdom.

Financial Disclosure(s):
The author(s) have made the following disclosure(s): M.B.: Advisory Board - Roche; Financial support - Bayer

C.D.: Consultant - Allergan, Bausch & Lomb, Laboratoires Théa, Novartis; Financial support - Laboratoires Théa

C.C.W.K.: Consultant - Bayer, Laboratoires Théa, Novartis

A.I.d.H.: Consultant - Ionis Pharmaceuticals, Gemini Therapeutics, Gyroscope Therapeutics, Roche

I.L.: Consultant - Optos Plc, Oxurion; Financial support - Optos Plc, Roche

T.P.: Consultant - Optos Plc, Bayer, Novartis; Financial support - Allergan, Alimera

J.M.: Board membership and Lecturer - Alcon, Allergan, Bayer, Kodiak, Novartis, Roche; Equity owner - Notal Vision, Ophthotech

Supported in part by the EYE-RISK Consortium; the European Union (Horizon 2020 Research and Innovation Programme grant no.: 634479). The funding organizations had no role in the design or conduct of this research.

HUMAN SUBJECTS: Human subjects were included in this study. The human ethics committees at each site approved the study. All research adhered to the tenets of the Declaration of Helsinki. All participants provided informed consent.

No animal subjects were included in this study.

Author Contributions:

Conception and design: Biarnés, Colijn, Verzijden, Meester-Smoor, Delcourt, Klaver, den Hollander, Lengyel, Peto, Monés

Analysis and interpretation: Biarnés, Colijn, Sousa, Ferraro, Garcia, Verzijden, Meester-Smoor, Delcourt, Klaver, den Hollander, Lengyel, Peto, Monés

Data collection: Biarnés, Colijn, Ferraro, Garcia, Verzijden, Meester-Smoor, Delcourt, Klaver, den Hollander, Monés

Obtained funding: EYE-RISK Consortium

Overall responsibility: Biarnés, Colijn, Sousa, Ferraro, Garcia, Verzijden, Meester-Smoor, Delcourt, Klaver, den Hollander, Lengyel, Peto, Monés

Abbreviations and Acronyms:
AMD = age-related macular degeneration; **CFP** = color fundus photography; **cvAUC** = cross-validated area under the receiver operating characteristic curve; **ECM** = extracellular matrix; **GA** = geographic atrophy; **GRS** = genetic risk score; **IQR** = interquartile range; **ROC** = receiver operating characteristic; **RPD** = reticular pseudodrusen; **RPE** = retinal pigment epithelium; **SD-OCT** = spectral-domain optical coherence tomography; **SNP** = single nucleotide polymorphism.

Correspondence:
Marc Biarnés, MPH, PhD, Barcelona Macula Foundation, C/Horaci 41-43, Esc B, 08022 Barcelona, Spain. E-mail: mbiarnes@barcelonamaculafound.org.